

Supporting Information

Cerebrosides of the Halotolerant Fungus *Alternaria raphani* Isolated from a Sea Salt Field

Wenliang Wang, Yi Wang, Hongwen Tao, Xiaoping Peng, Peipei Liu, and Weiming

Zhu^{*}

*Key Laboratory of Marine Drugs, Chinese Ministry of Education, School of Medicine and
Pharmacy, Ocean University of China, Qingdao 266003, Peoples' Republic of China*

List of Supporting Information

Bioassay Protocols	S3
The 18S rRNA sequence data of <i>Alternaria raphani</i> THW-18.....	S4
Figure S1. X-ray crystal structure of bisdethiobis(methylthio)acetylaranotin (6).....	S5
Figure S2. The ¹ H-NMR spectrum of alternaroside A (1) in <i>d</i> ₆ -DMSO.....	S6
Figure S3. The ¹³ C-NMR spectrum of alternaroside A (1) in <i>d</i> ₆ -DMSO.....	S7
Figure S4. The ¹ H-NMR spectrum of alternaroside B (2) in <i>d</i> ₆ -DMSO.....	S8
Figure S5. The ¹³ C-NMR spectrum of alternaroside B (2) in <i>d</i> ₆ -DMSO.....	S9
Figure S6. The ¹ H-NMR spectrum of alternaroside C (3) in <i>d</i> ₆ -DMSO.....	S10
Figure S7. The ¹³ C-NMR spectrum of alternaroside C (3) in <i>d</i> ₆ -DMSO.....	S11
Figure S8. The ¹ H-NMR spectrum of alternarosin A (4) in <i>d</i> ₆ -DMSO.....	S12
Figure S9. The ¹³ C-NMR spectrum of alternarosin A (4) in <i>d</i> ₆ -DMSO.....	S13
Figure S10. The positive-ion ESIMS/MS spectrum of alternaroside A (1).....	S14
Figure S11. The positive-ion ESIMS/MS spectrum of alternaroside B (2).....	S15

Figure S12. The positive-ion ESIMS/MS spectrum of alternaroside C (3).....	S16
Figure S13. GC/MS of methyl 2-hydroxyoctadec-3-enoate (t_R 16.81 min) from methanolysis of alternaroside A (1).....	S17
Figure S14. GC/MS of methyl 2-hydroxyoctadec-3-enoate (t_R 16.81 min) from methanolysis of alternaroside B (2).....	S18
Figure S15. GC/MS of methyl 2-hydroxyoctadec-3-enoate (t_R 16.81 min) from methanolysis of alternaroside C (3).....	S19
Figure S16. Elucidation by positive-ion ESIMS/MS of alternaroside A (1).....	S20
Figure S17. Elucidation by positive-ion ESIMS/MS of alternaroside B (2).....	S21
Figure S18. Elucidation by positive-ion ESIMS/MS of alternaroside C (3).....	S22

Bioassay Protocols

Cytotoxic Assays. In the MTT assay, cell lines were grown in RPMI-1640 supplemented with 10% FBS under a humidified atmosphere of 5% CO₂ and 95% air at 37 °C. Cell suspensions, 200 µL, at a density of 5×10^4 cell mL⁻¹ were plated in 96-well microtiter plates and incubated for 24 h. Then, 2 µL of the test solutions (in MeOH) were added to each well and further incubated for 72 h. The MTT solution (20 µL, 5 mg/mL in RPMI-1640 medium) was then added to each well and incubated for 4 h. Old medium containing MTT (150 µL) was then gently replaced by DMSO and pipetted to dissolve crystals formed. Absorbance was then determined on a Spectra Max Plus plate reader at 540 nm. In the SRB assay, 200 µL of the cell suspensions were plated in 96-well plates at a density of 2×10^5 cell mL⁻¹. Then 2 µL of the test solutions (in MeOH) was added to each well and the culture was further incubated for 24 h. The cells were fixed with 12% trichloroacetic acid and the cell layer stained with 0.4% SRB. The absorbance of the SRB solution was measured at 515 nm. The new isolates **1–4** were evaluated for cytotoxicity against P388 and HL-60 cancer cells with the SRB method,²⁵ and the A549 and BEL-7402 cancer cells with the MTT methods.²⁶ Vp-16 (etoposide) was used as the positive control with the IC₅₀ values of 0.050 µM, 0.042 µM, 0.63 µM, and 1.03 µM, respectively.

Antimicrobial Assays. According to agar dilution method,²⁷ the tested strains (*Escherichia coli*, *Bacillus subtilis*) were cultivated in LB agar plates for bacteria and in YPD agar plates for *C. albicans* at 37 °C. Ciprofloxacin lactate and fluconazol was used as the positive control for bacteria and *Candida albicans* with MIC values of 3.71 µM, 7.42 µM, and 5.10 µM, respectively. Compounds **1–4** and positive controls were dissolved in 5% DMSO-H₂O at different concentrations from 400 to 0.78 µg/mL by the continuous 2-fold dilution methods. A 5 µL quantity of test solution was absorbed by a paper disk (5 mm diameter) and placed on the assay plates. After 24 h incubation, zones of inhibition (mm in diameter) were recorded. The minimum inhibitory concentrations (MICs) were defined as the lowest concentration at which no microbial growth could be observed.

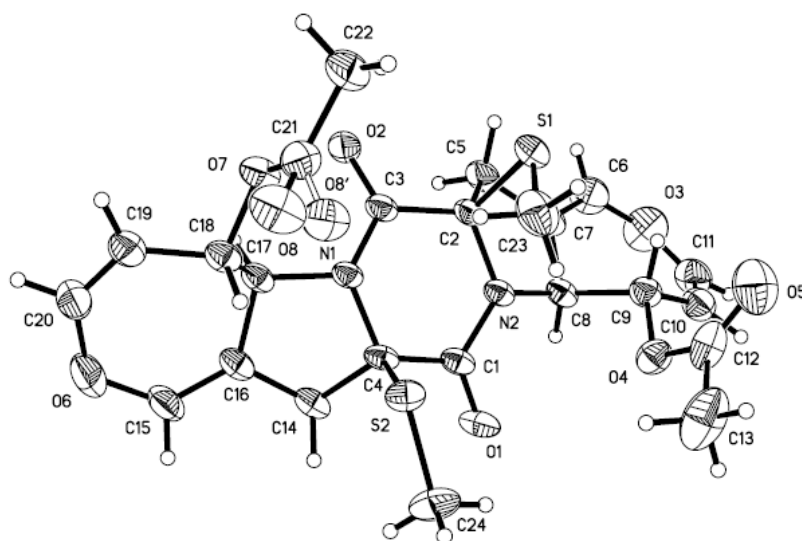
Antioxidative Assays. According to DPPH assay,²⁸ 160 µL of reaction mixtures containing test samples and 40 µL of DPPH (Sigma) in MeOH were plated in 96-cell plates and incubated in the dark for 30 min. After the reaction, absorbance was measured at 520 nm, and percent inhibition was calculated. The antioxidant activity of each sample was expressed in terms of IC₅₀ (the

concentration of sample required to scavenge 50% of DPPH free radicals) and calculated from the log-dose inhibition curve. Ascorbic acid was used as the positive control with IC₅₀ 22 μ M.

The 18S rRNA sequence data of *Alternaria raphani* THW-18

```
TTATACCGTGAAACTGCGAATGGCTCATTAAATCAGTTATCGTTTATTTGATAATACCTTACTAC
TTGGATAACCGTGGTAATTCTAGAGCTAATACATGCTGAAAATCCCGACTTCGGAAGGGATGTGT
TTATTAGATAAAAAACCAATGCCCTTCGGGGCTTTTTGGTGATTCATGATAACTTTACGGATCGC
ATAGCCTTGCGCTGGCGACGGTTCATTCAAATTTCTGCCCTATCAACTTTTCGATGGTAAGGTATT
GGCTTACCATGGTTTCAACGGGGTAACGGGGAATTAGGGTTCGATTCCGGAGAGGGAGCCTGAGAA
ACGGCTACCACATCCAAGGAAGGCAGCAGGCGCGCAAATTACCCAATCCCGACACGGGGAGGTAG
TGACAATAAATACTGATACAGGGCTCTTTTGGGTCTTGTAATTGGAATGAGTACAATTTAAACCT
CTTAACGAGGAACAATTGGAGGGCAAGTCTGGTGCCAGCAGCCGCGTAATTCCAGCTCCAATAG
CGTATATTAAAGTTGTTGCAGTTAAAAAGCTCGTAGTTGAAACTTGGGCCTGGCTGGCGGGTCCG
CCTCACCGCGTGCACTCGTCCGGCCGGGCCTTCCTTCTGAAGAACCTCATGCCCTTCACTGGGCG
TGCTGGGGAATCAGGACTTTTACTTTGAAAAAATTAGAGTGTTCAAAGCAGGCCTTTGCTCGAAT
ACGTTAGCATGGAATAATAAAATAGGGCGTGCGTTTCTATTTTGTGGTTTCTAGAGACGCCGCA
ATGATTAACAGGAACAGTCGGGGGCATCAGTATTCAGTTGTCAGAGGTGAAATTCTTGGAATTTAC
TGAAGACTAACTACTGCGAAAGCATTTGCCAAGGATGTTTTTATTAATCAGTGAACGAAAGTTAG
GGGATCGAAGACGATCAGATACCGTCGTAGTCTTAACCGTAACTATGCCGACTAGGGATCGGGC
GATGTTCTTTTTCTGACTCGCTCGGCACCTTACGAGAAATCAAAGTTTTTGGGTTCGGGGGGAT
TATGGTCGCAAGGCTGAACTTAAAGAAATTGACGGAAGGTCACCACCAGGCGTGGAGCCTGCGG
CTTAATTTGACTCAACACGGGGAACTCACCAGGTCCAGATGAAATAAGGATTGACAGATTGAGA
GCTCTTTCTTGATTTTTTCAAGGTGGTGGTGCATGGCCGTTCTTAGTTTCGTGGGGTGACTTGTCTGC
TTAaTTgCGATAACGAGCGAGACCTTACTCTGCTAAATAGCCAGGCTAACTTTGGTTGGTCGCCG
GCTTCTTAGAGAGACTATCAACTCAAGTTGATGGAAGTTTGAGGCAATAACAGGTCTGTGATGCC
CTTAGATGTTCTGGGCCGCACGCGCGCTACACTGACAGAGCCAACGAGTTCTTTTCCTTGTTTGA
AAGAATTGGGTAATCTTGTTAACTCTGTCGTGCTGGGGATAAAGCATTGCAATTATTGCTTTTC
AACGAGGAATGCCTAGTAAGCGCGTGTATCAGCATGCGTTGATTACGTCCCTGACCTTTGTACA
CACCGCCCGTCGCTACTACCGATTGAATGGCTCAGTGAGGCCTTCGGAAGTGGCTCGAGGAGGTTG
GCAACGACCACCTCAAGCCGAAAGTTCGTCAAACCTCGG
```

Figure S1. X-ray crystal structure of bisdethiobis(methylthio)acetylaranotin (**6**)



X-ray crystal structure analysis of bisdethiobis(methylthio)acetylaranotin (6**):** colorless block crystal of $C_{24}H_{26}N_2O_8S_2$. Space group $P\ 2(1)$, $a = 9.4623(12)\ \text{\AA}$, $b = 12.9379(16)\ \text{\AA}$, $c = 10.97900(13)\ \text{\AA}$, $\alpha = 90.00^\circ$, $\beta = 110.758(2)$, $\gamma = 90.00^\circ$, $V = 1256.8(2)\ \text{\AA}^3$, $Z = 2$, crystal size $0.50 \times 0.47 \times 0.46\ \text{mm}^3$. A total of 3094 unique reflections ($2\theta < 50^\circ$) were collected using graphite monochromated MoK α ($\lambda = 0.71073\ \text{\AA}$) on a CCD area detector diffractometer. The structure was solved by direct methods (SHELXS-97) and expanded using Fourier techniques. The final cycle of full-matrix least squares refinement was based on 3094 unique reflections ($2\theta < 50^\circ$) and 325 variable parameters and converged with unweighted and weighted agreement factors of $R = 0.0442$, $R_w = 0.0995$ and $R_1 = 0.0387$ for $I > 2\sigma(I)$ data. Crystallographic data excluding structure factors for structure **6** in this paper have been deposited with the Cambridge Crystallographic Data Centre as supplementary publication number CCDC 725712. Copies of the data can be obtained, free of charge, on application to CCDC, 12 Union Road, Cambridge CB2 1EZ, UK [fax: +44 (0) 1223336033 or e-mail: deposit@ccdc.cam.ac.uk]

Figure S2. The ^1H -NMR spectrum of alternaroside A (**1**) in d_6 -DMSO

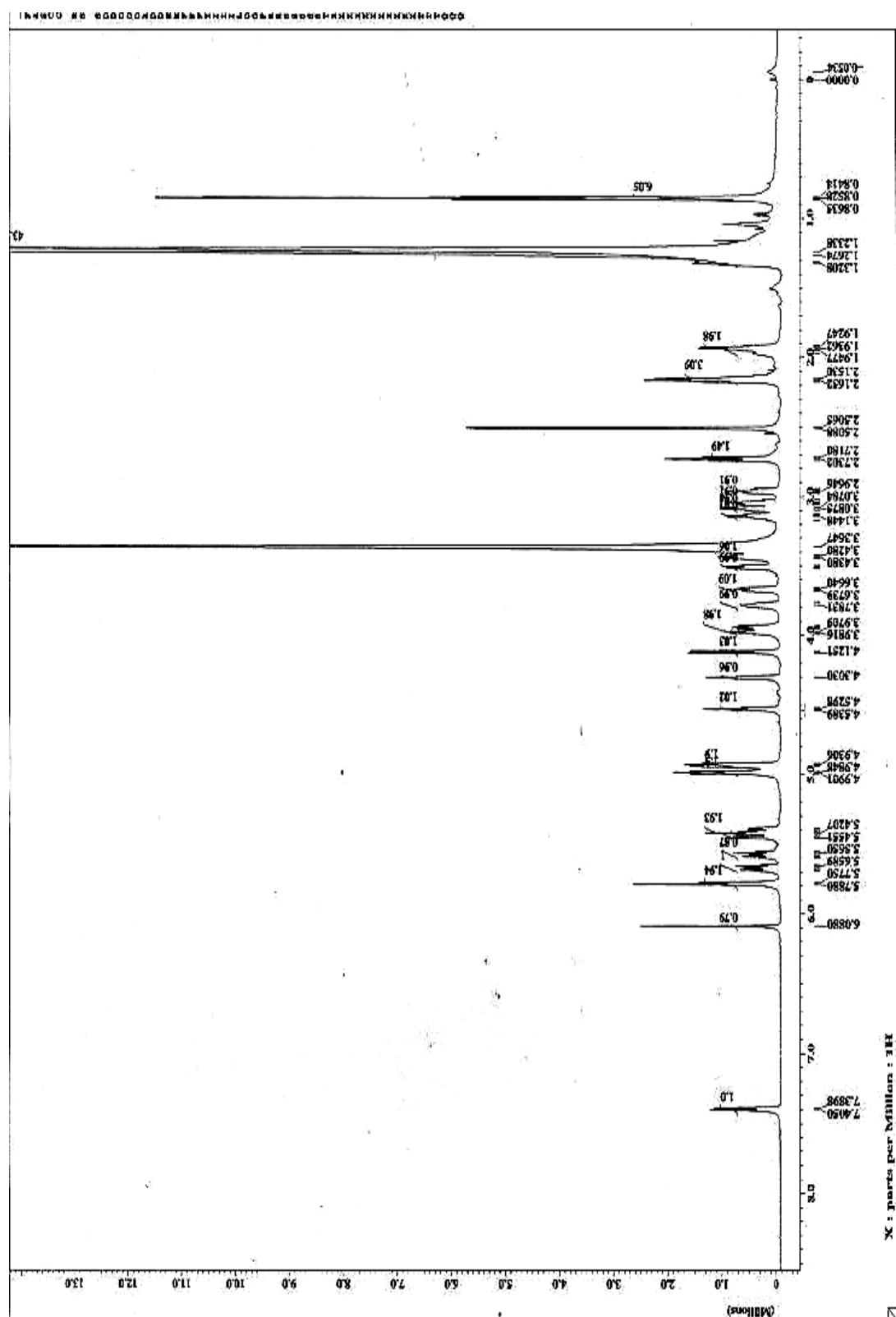


Figure S3. The ^{13}C -NMR spectrum of alternaroside A (**1**) in d_6 -DMSO

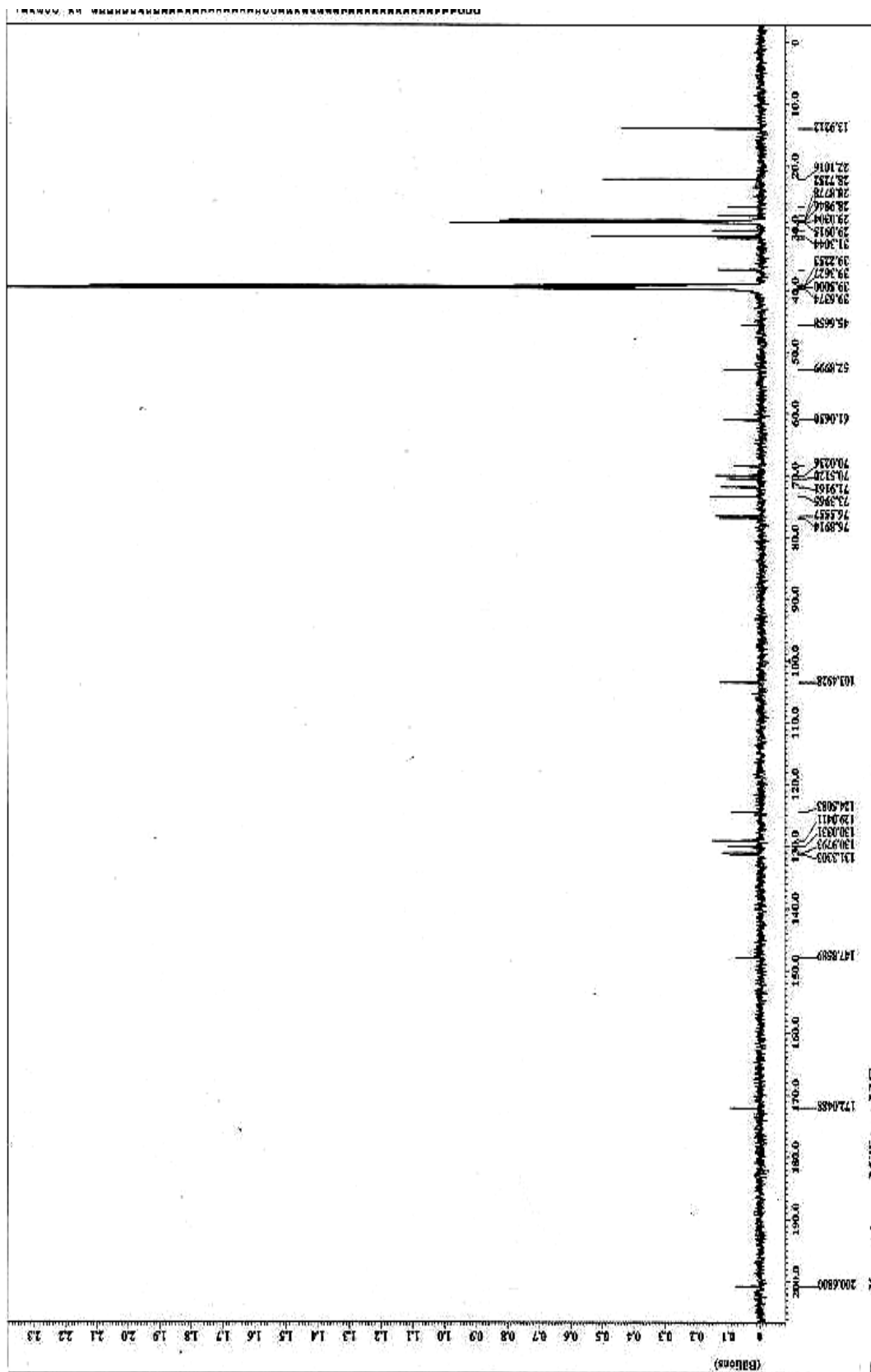


Figure S4. The ^1H -NMR spectrum of alternaroside B (**2**) in d_6 -DMSO

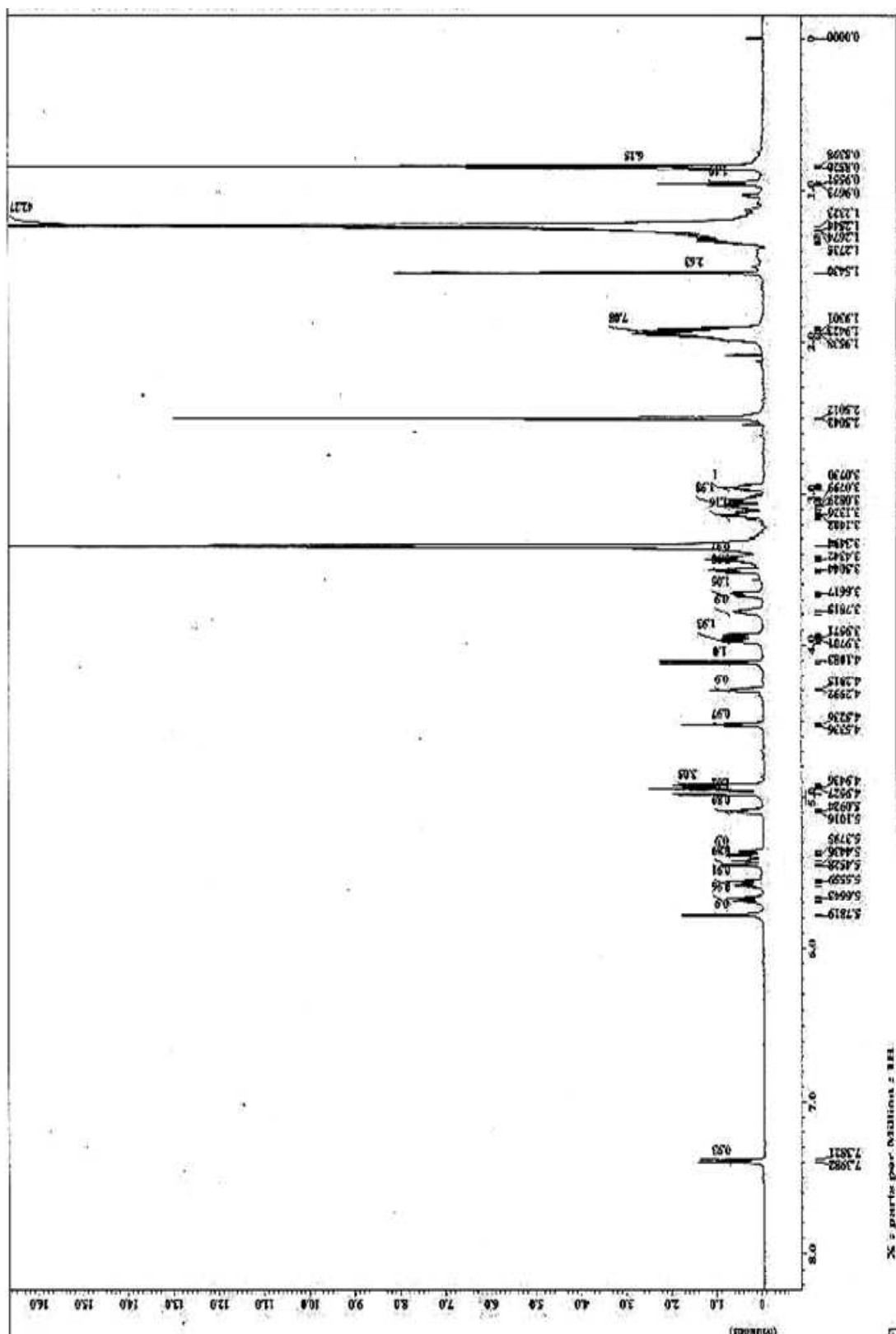


Figure S5. The ^{13}C -NMR spectrum of alternaroside B (**2**) in d_6 -DMSO

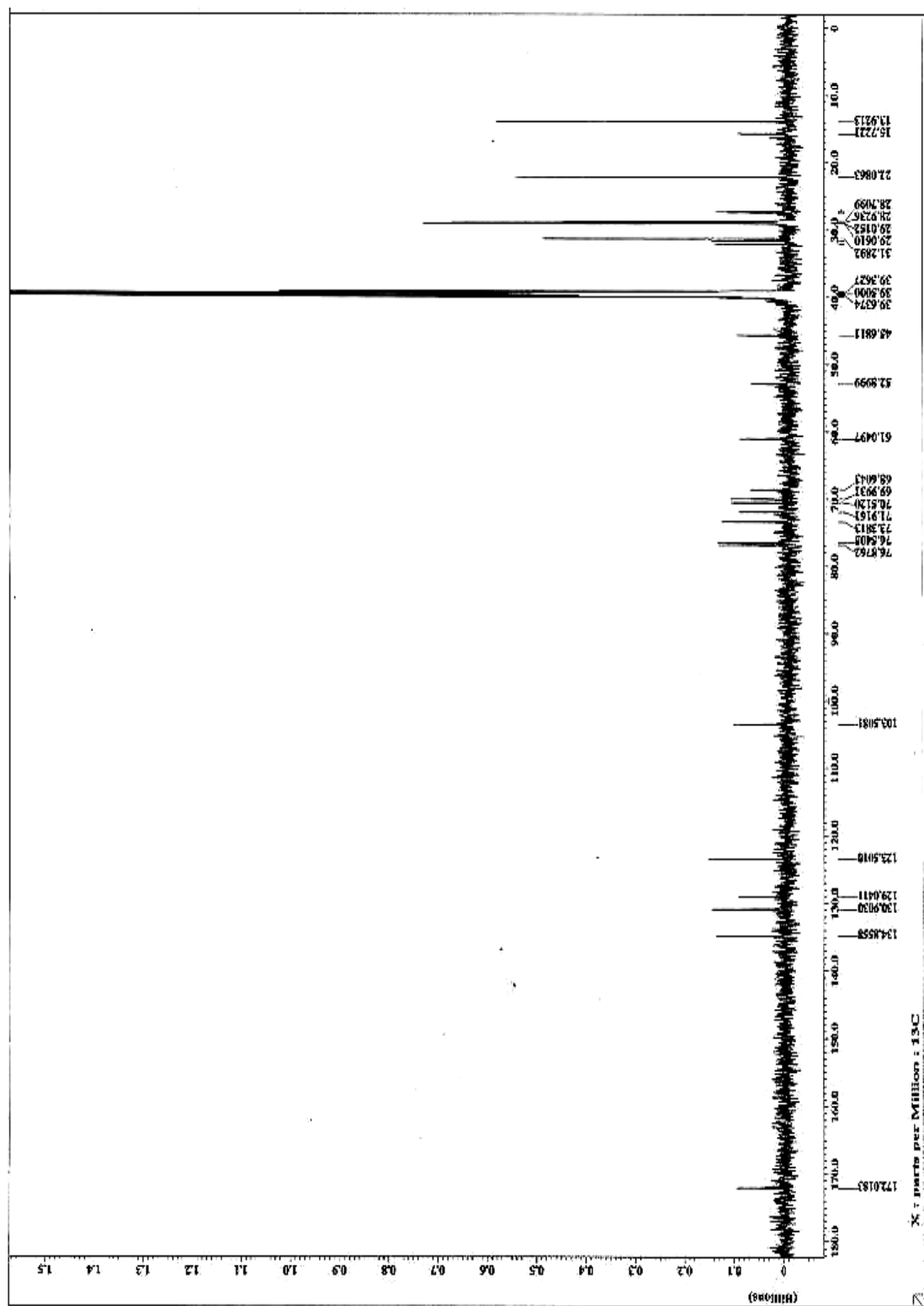


Figure S6. The ^1H -NMR spectrum of alternaroside C (**3**) in d_6 -DMSO

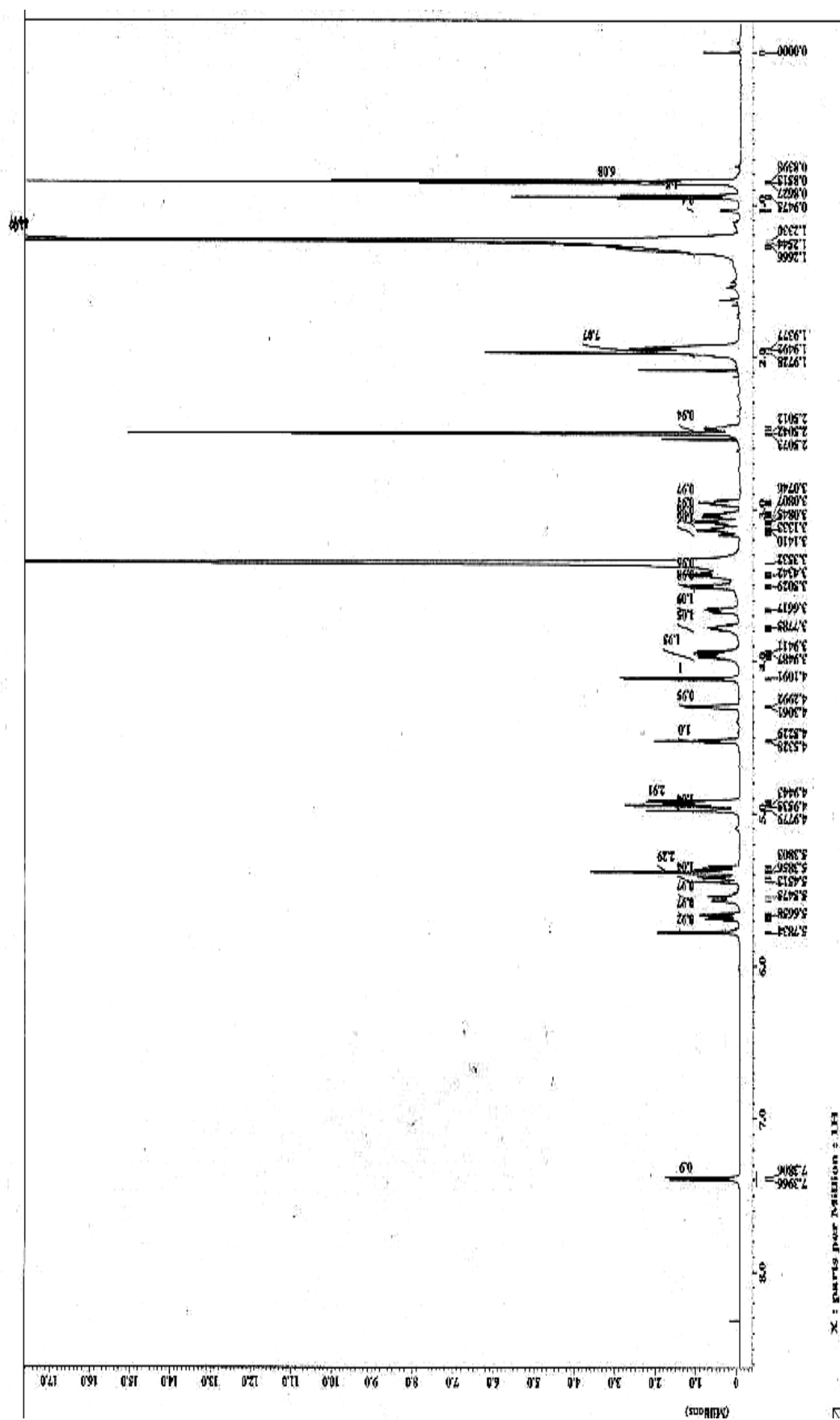


Figure S7. The ¹³C-NMR spectrum of alternaroside C (3) in d₆-DMSO

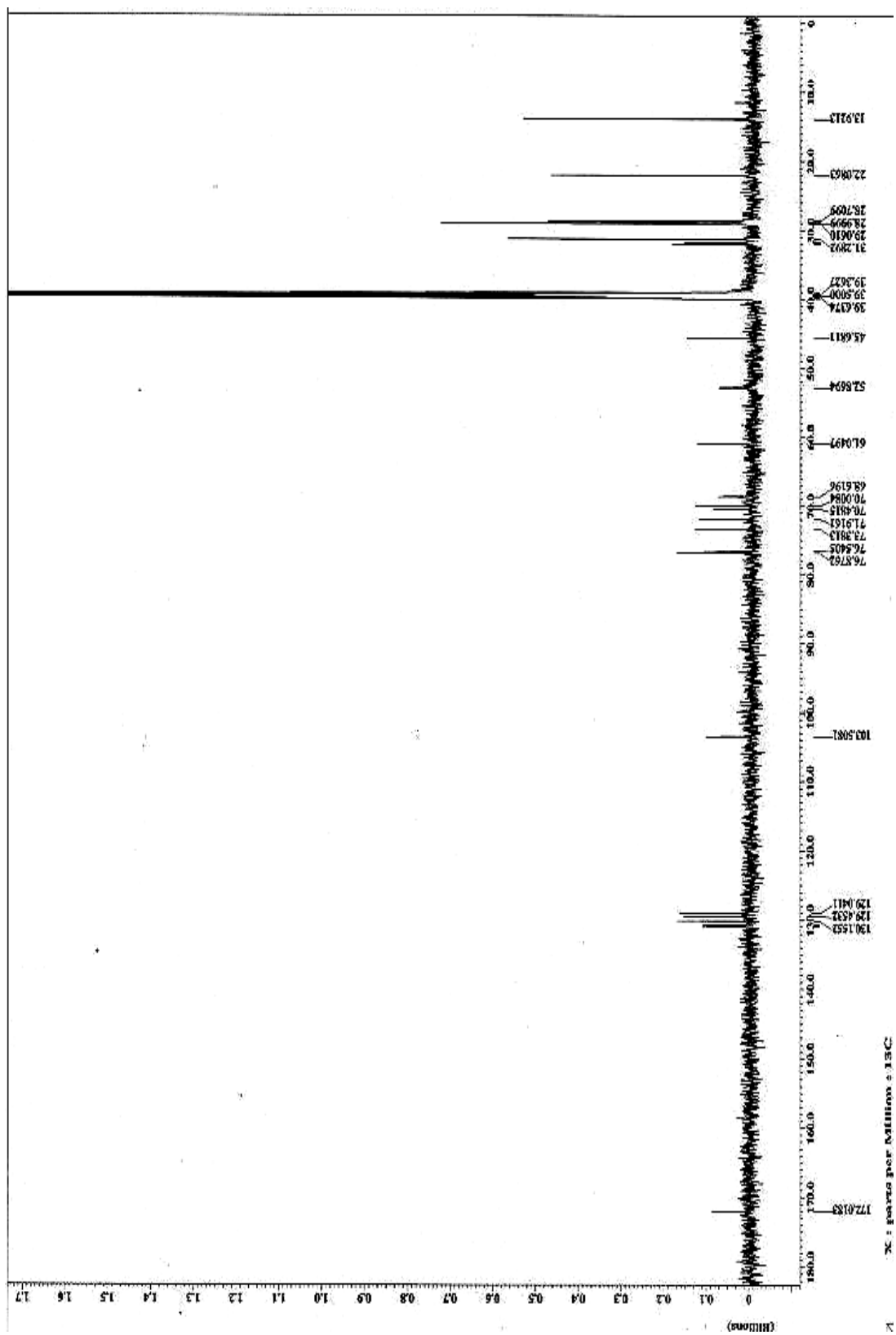


Figure S8. The ^1H -NMR spectrum of alternarosin A (**4**) in d_6 -DMSO

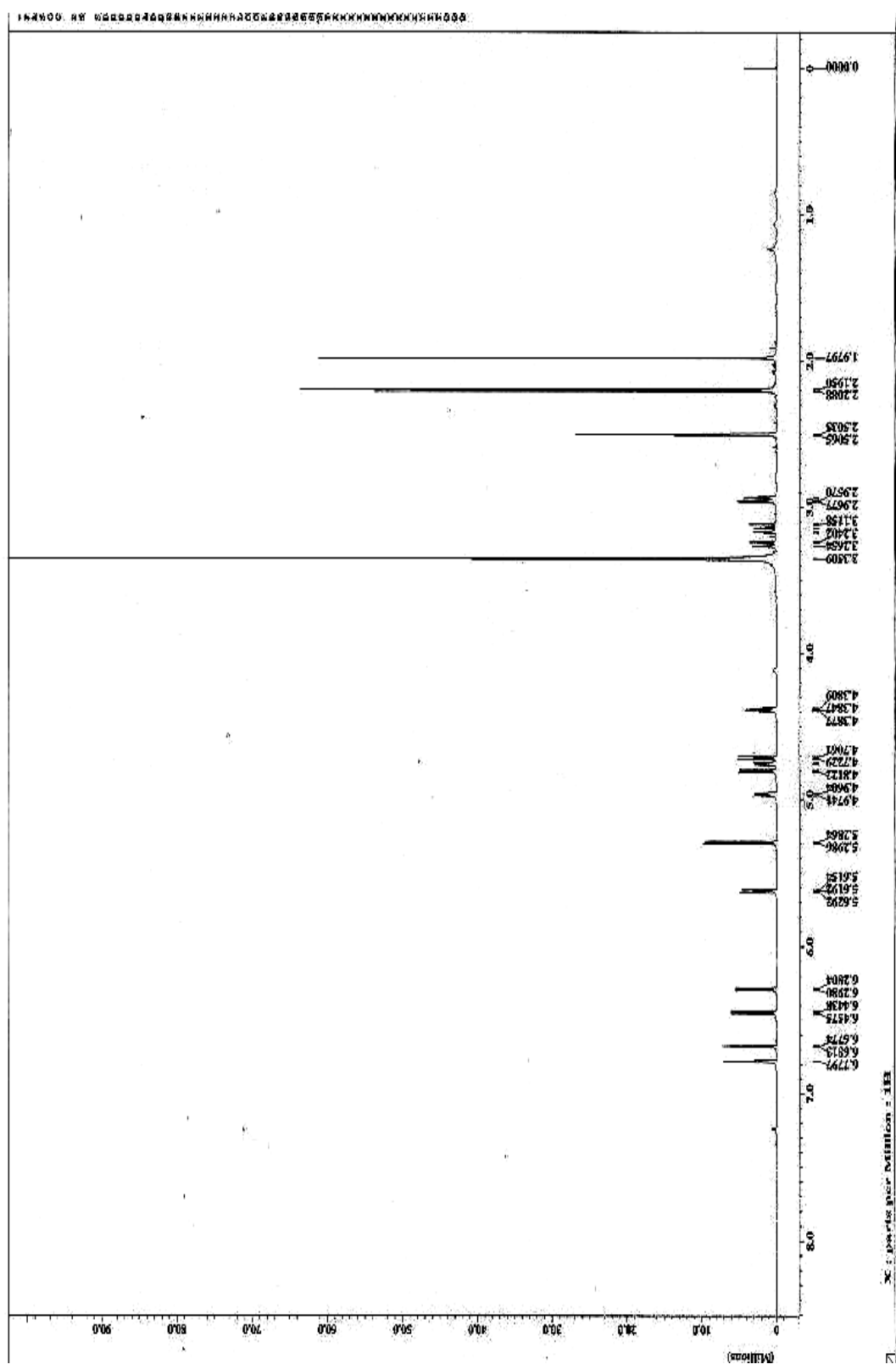


Figure S9. The ^{13}C -NMR spectrum of alternarosin A (**4**) in d_6 -DMSO

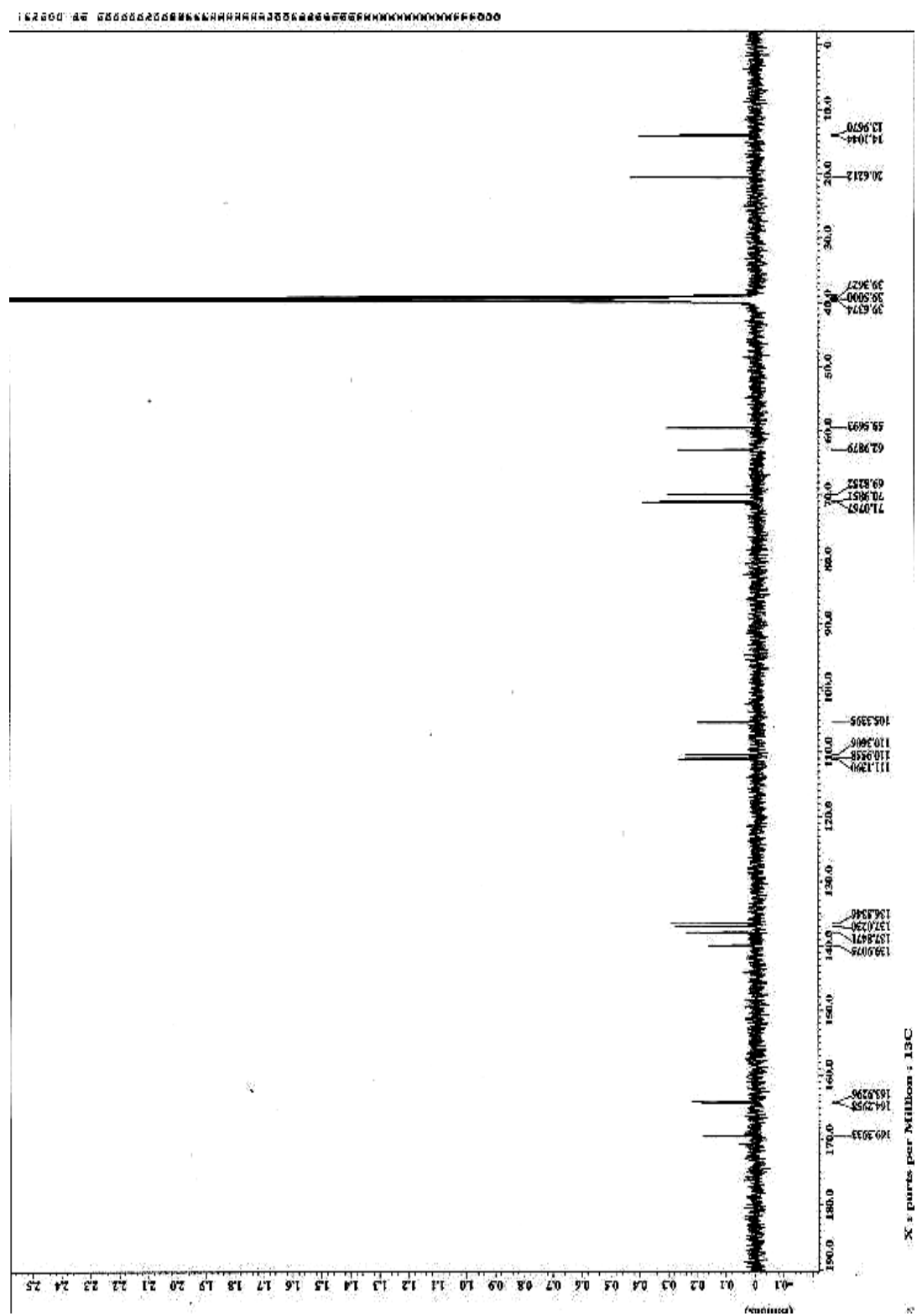


Figure S10. The positive-ion ESIMS/MS spectrum of alternaroside A (1)

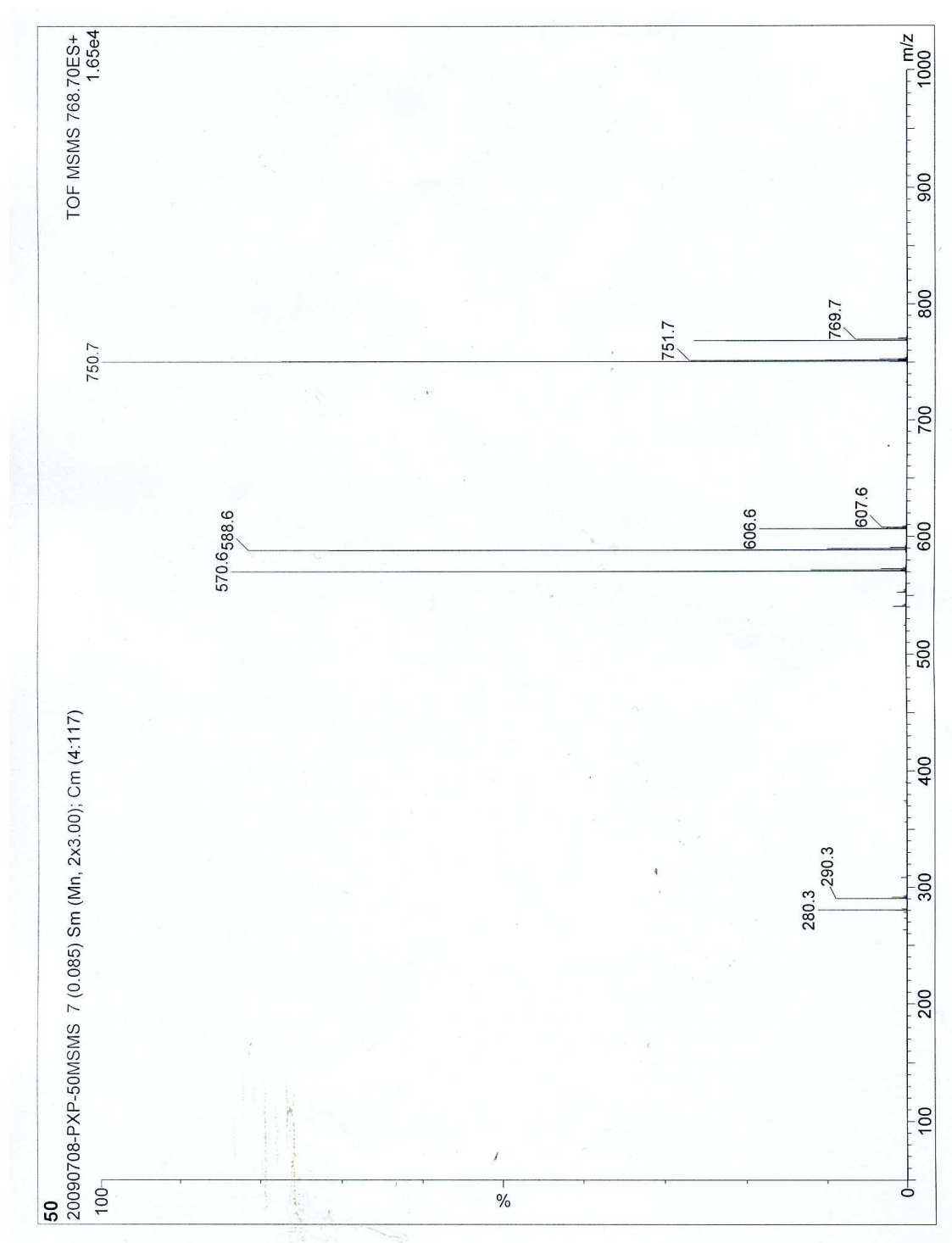


Figure S11. The positive-ion ESIMS/MS spectrum of alternaroside B (2)

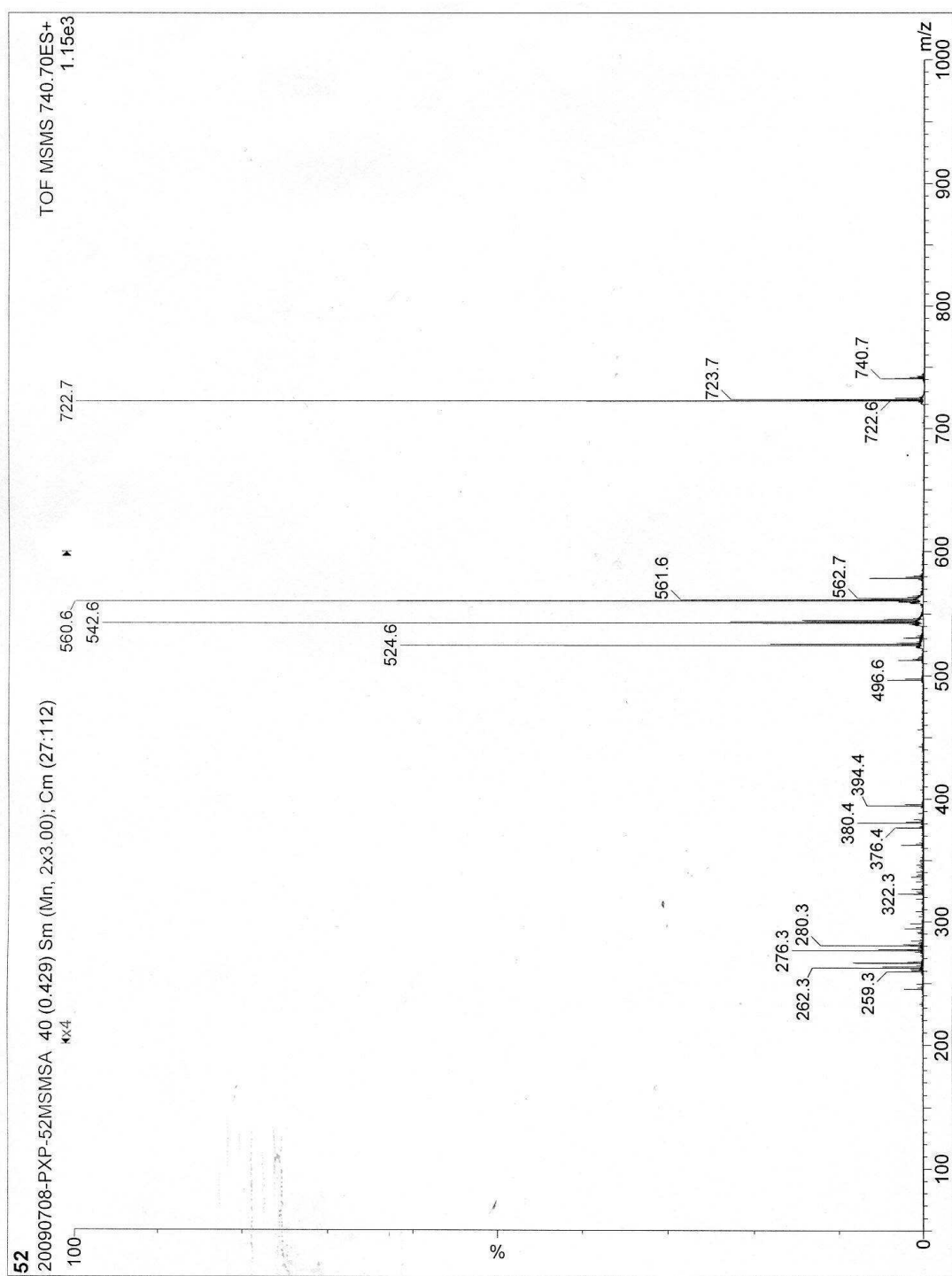


Figure S13. GC/MS of methyl 2-hydroxyoctadec-3-enoate (t_R 16.81 min) from

methanolysis of alternaroside A (1)

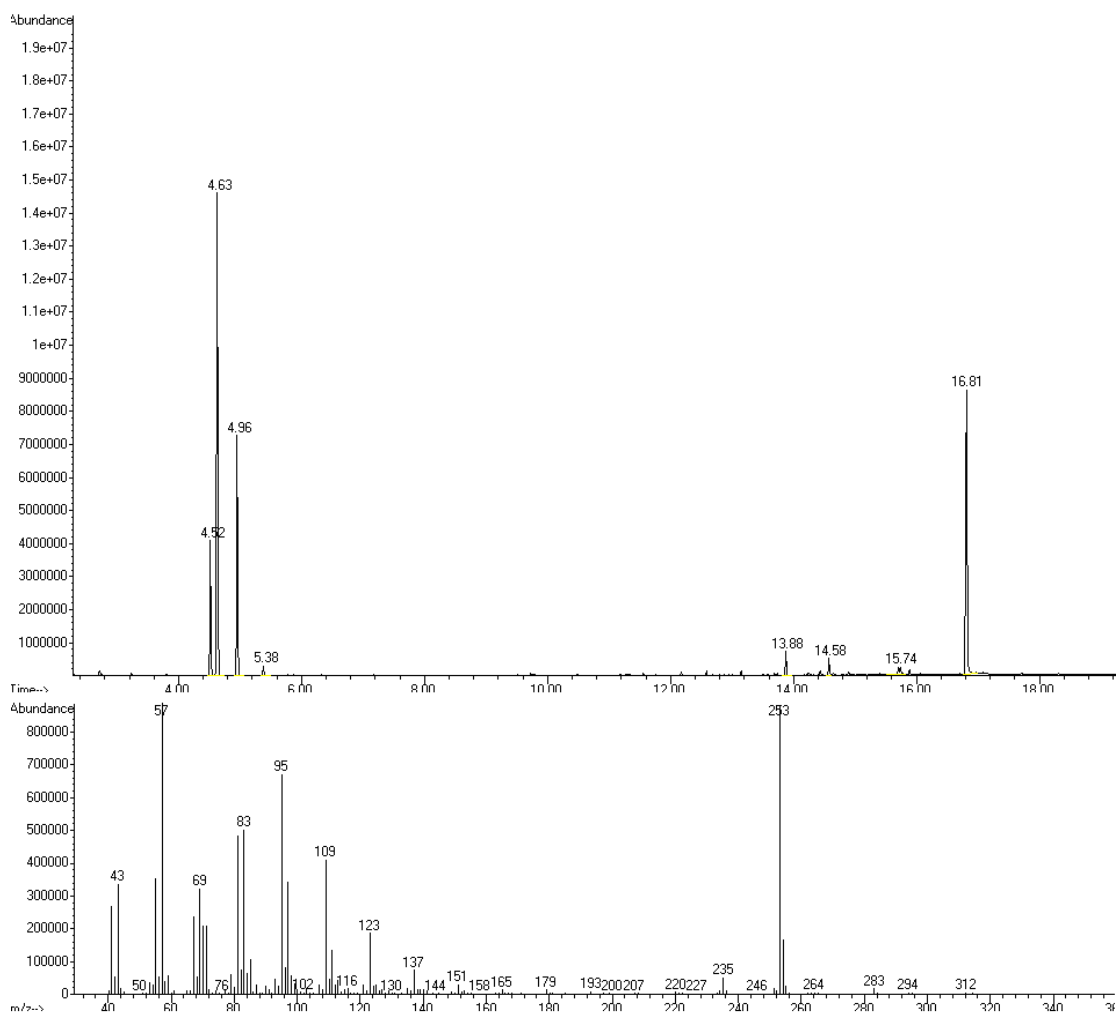


Figure S14. GC/MS of methyl 2-hydroxyoctadec-3-enoate (t_R 16.81 min) from

methanolysis of alternaroside B (2)

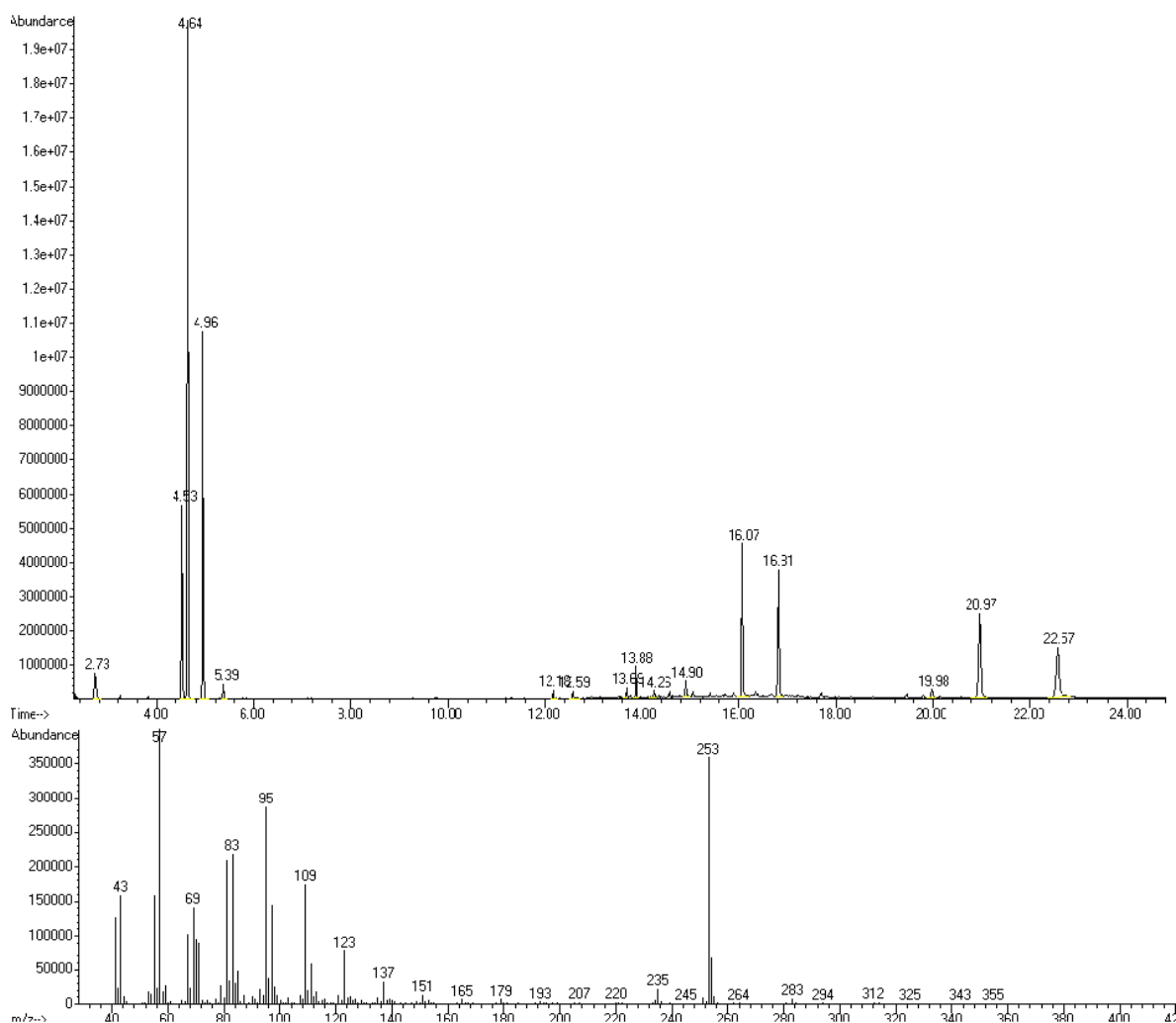


Figure S15. GC/MS of methyl 2-hydroxyoctadec-3-enoate (t_R 16.81 min) from

methanolysis of alternaroside C (3)

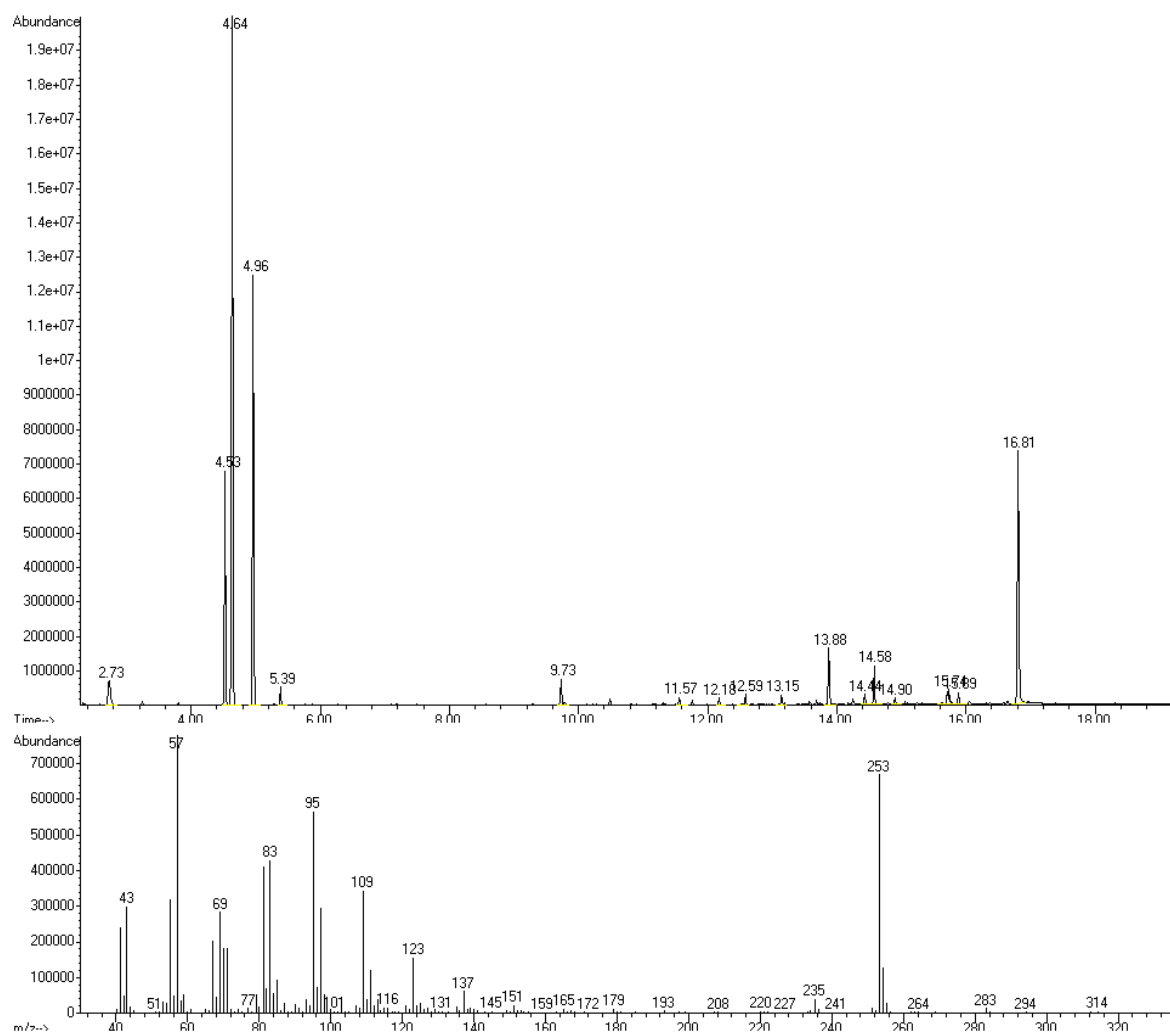


Figure S16. Elucidation by positive-ion ESIMS/MS of alternaroside A (1)

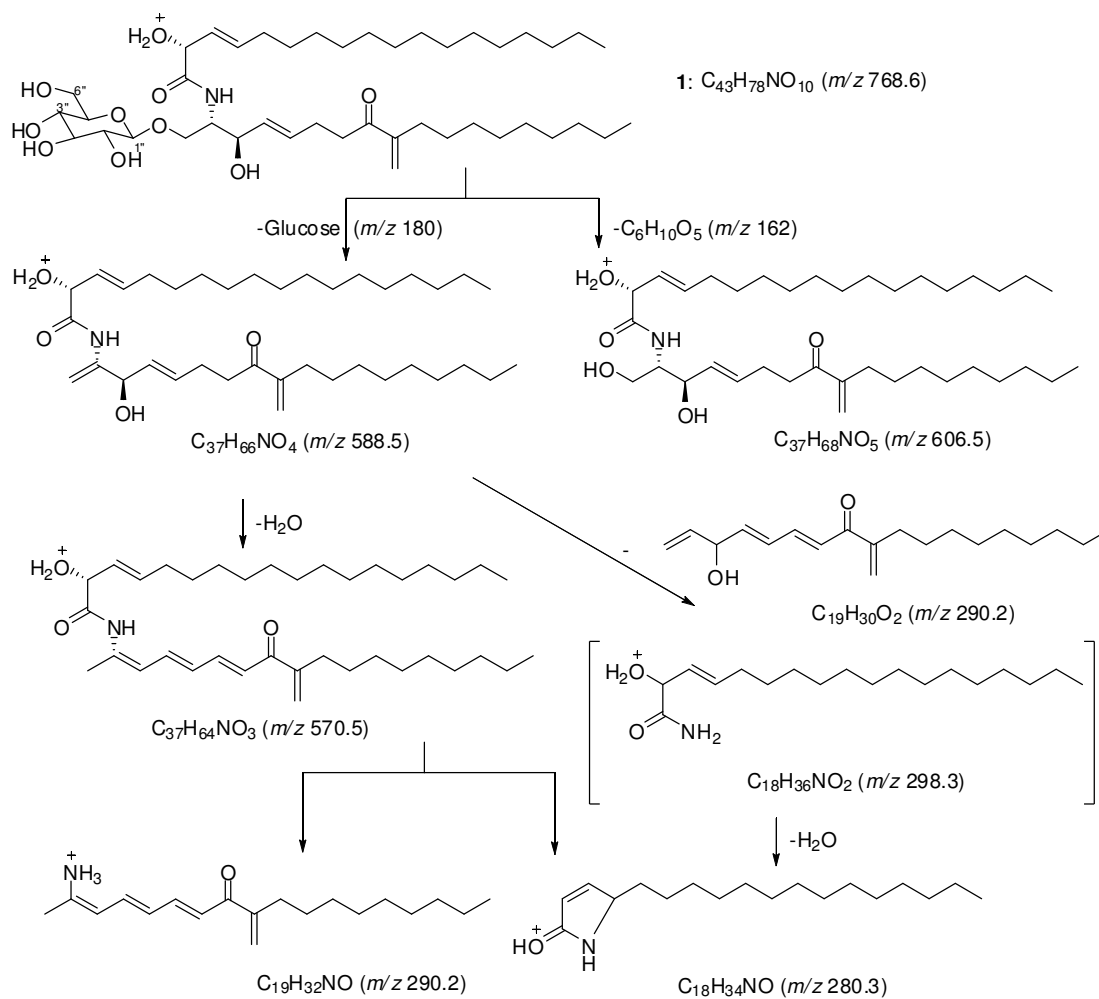


Figure S17. Elucidation by positive-ion ESIMS/MS of alternaroside B (**2**)

